THE JOURNAL OF BIOLOGICAL CHEMISTRY
Vol. 277, No. 40, Issue of October 4, pp. 37582–37589, 2002

Printed in U.S.A.

Membrane-Protein Interactions Contribute to Efficient 27-Hydroxylation of Cholesterol by Mitochondrial Cytochrome P450 27A1*

Received for publication, May 17, 2002, and in revised form, July 16, 2002
Published, JBC Papers in Press, July 17, 2002, DOI 10.1074/jbc.M204909200

Dilyara Murtazina‡, Andrei V. Puchkaev‡§, Catherine H. Schein¶, Numan Oezguen¶, Werner Braun¶, Amit Nanavati‡ ‡‡, and Irina A. Pikuleva‡‖

From the ‡Department of Pharmacology and Toxicology and ¶Sealy Center for Structural Biology, Department of Human Biological Chemistry and Genetic, University of Texas Medical Branch, Galveston, Texas 77555

Mitochondrial cytochrome P450 27A1 (P450 27A1) catalyzes 27-hydroxylation of cholesterol, the first step in the alternative bile acid biosynthetic pathway. Although several crystal structures of P450s are known, no structural information is available for the mammalian, membrane-bound enzymes involved in the removal of cholesterol from the body. We prepared a three-dimensional model of P450 27A1 based on the structure of P450 BM-3. Conservative and non-conservative mutations were introduced at hydrophobic and positively charged residues in the putative F-G loop and the adjacent helix G (positions 219–237). Subcellular distribution of the mutant P450s expressed in *Escherichia coli* was used as a measure of membrane-protein interactions. Conservative substitutions of residues located on the surface, according to our model, L219V, L219I, Y220F, F223Y, L224I, R229K, V231L, F234Y, K236R, and R237K, weakened the association of the mutant P450s with the membrane and led to the appearance of up to 21% of P450 27A1 in the bacterial cytosol. It is likely that the mutated side chains are involved in binding to membrane phospholipids. Substitutions in the F-G loop did not significantly affect the K_m value for cholesterol hydroxylation. However, non-conservative mutants, L219N, Y220A, Y220S, F223A, K226R, and R229A, had significantly impaired catalytic properties, indicating strict requirements for the size and polarity of the side chains at these positions for the catalysis. The results provide insight into the membrane topology of mitochondrial P450s and indicate the importance of membrane-protein interactions in the efficiency of reactions catalyzed by P450 27A1.

Conversion of cholesterol into bile acids is the principal route of cholesterol removal from the body in mammals (1). Cholesterol is degraded to bile acids either through the classical (hepatic) or alternative (extrahepatic) bile acid biosynthetic pathways, involving several cytochrome P450 (P450)[1] enzymes. P450 7A1 catalyzes 7α-hydroxylation of cholesterol, the first and rate-limiting step in the classical bile acid biosynthetic pathway (2, 3), whereas P450 27A1 carries out 27-hydroxylation of cholesterol, the first step in the alternative bile acid biosynthesis (4, 5). P450 27A1 also catalyzes multiple oxidation reactions at the C-27 atom of bile acid intermediates in the classical bile acid biosynthetic pathway. P450 7A1 seems to be vital for life because no mutations have yet been identified in the gene for this protein. Mutations in P450 *27A1* gene correlate with a hereditary disease, cerebrotendinous xanthomatosis (CTX) (6), which is characterized by the abnormal deposition of cholesterol and cholestanol in body tissues. If untreated, CTX leads to tendon xanthomas, serious neurological defects, premature arteriosclerosis, osteoporosis, and even death (7). P450s 7A1 and 27A1 are membrane-bound proteins located in the endoplasmic reticulum and inner mitochondrial membrane, respectively. Both mitochondrial and microsomal members of the cytochrome P450 superfamily are proposed to have a similar mode of association with the membrane via a large hydrophilic domain anchored to the lipid bilayer through several noncontiguous portions of the polypeptide chain (8, 9). The membrane interacting areas have not yet been identified in mitochondrial P450s, and it is not clear at present whether they are the same in different enzymes. Microsomal P450s share at least one common membrane-binding site, an N-terminal signal anchor of about 20 amino acid residues. Another possible common site of association with the endoplasmic reticulum is an area between the F and G helices, the F-G loop (10–14). The F-G loop was also proposed to form a mouth of the channel that allows the substrate to pass from the surface of the P450 molecule to the buried active site (10, 11). Our recent studies indicate that membrane binding and substrate access merge in cholesterol-metabolizing enzyme, microsomal P450 7A1, and the putative F-G loop is simultaneously the site of attachment to membrane and cholesterol entry in this P450 (14). It is likely that another cholesterol-metabolizing enzyme, mitochondrial P450 27A1, also recruits cholesterol from the lipid bilayer, as neither the enzyme nor its substrate are soluble in the aqueous environment of the cell. Previously, we have studied the role of the putative helices F and G in P450 27A1, regions that flank the F-G loop (15). Our data indicate that the putative helices F and G form the sides of the of the substrate access channel in this P450, and residues lining the interior of the channel control the orientation of the substrate as it enters

* This work was supported by United States Public Health Service Grant GM62882-01 (to I. A. P.), Department of Energy Grant DE-FG03-00ER63041 (to W. B.), the Texas Higher Education Coordinating Board Grant ARP 004952-0084-1999 (to W. B.), the John Sealy Memorial Endowment Funds 2535-01 (to W. B.) and 2543-00 (to I. A. P.), and Center Grant ES06676. The costs of publication of this article were defrayed in part by the payment of page charges. This article must therefore be hereby marked "*advertisement*" in accordance with 18 U.S.C. Section 1734 solely to indicate this fact.

The atomic coordinates and structure factors (code IMFX) have been deposited in the Protein Data Bank, Research Collaboratory for Structural Bioinformatics, Rutgers University, New Brunswick, NJ (http://www.rcsb.org/).

§ Present address: Institute of Bioorganic Chemistry, National Academy of Sciences of Belarus, Minsk 220141, Belarus.

‡‡ Participant in the Summer Undergraduate Research Program at the University of Texas Medical Branch.

‖ To whom correspondence should be addressed. Tel.: 409-772-9657; Fax: 409-772-9642; E-mail: irpikule@utmb.edu.

[1] The abbreviations used are: P450, cytochrome P450; CTX, cerebrotendinous xanthomatosis; PDB, protein data base.

TABLE I
Oligonucleotides and templates used to generate P450s 27A1 mutants

Template	Mutation	Oligonucleotides
Wild type	L219N	5′-GGGTTAATGTTCCAGAATTCAAACTATGCCACCTTC-3′[a] 5′-GAAGGTGGCATAGTTTGAATTCTGGAACATTAACCC-3′
Wild type	L219V	5′-GGGTTAATGTTCCAGAACTCAGTATACGCCACCTTCCTCCCC-3′ 5′-GGGGAGGAAGGTGGCGTATACTGAATTCTGGAACATTAACCC-3′
Wild type	L219I	5′-GGGTTAATGTTCCAGAACTCAATCTATGCCACCTTCCTCCCC-3′ 5′-GGGGAGGAAGGTGGCATAGATTGAGTTCTGGAACATTAACCC-3′
Wild type	Y220A	5′-TTAATGTTCCAGAACTCACTCGCTGCCACCTTCCTCCCC-3′ 5′-GGGGAGGAAGGTGGCAGCGAGTGAGTTCTGGAACATTAA-3′
Wild type	Y220S	5′-ATGTTCCAGAACTCACTCAGCGCTACCTTCCTCCCC-3′ 5′-GGGGAGGAAGGTAGCGCTGAGTGAGTTCTGGAACAT-3′
Wild type	Y220F	5′-ATGTTCCAGAACTCACTCTTTGCCACCTTCCTCCCC-3′ 5′-GGGGAGGAAGGTGGCAAAGAGTGAGTTCTGGAACAT-3′
Wild type	F223A	5′-AACTCACTCTATGCCACAGCGCTCCCCAAGTGG-3′ 5′-CCACTTGGGGAGCGCTGTGGCATAGAGTGAGTT-3′
Wild type	F223L	5′-CAGAACTCACTCTATGCCACCCTCCTCCCCAAGTGGACT-3′ 5′-AGTCCACTTGGGGAGGAGGGTGGCATAGAGTGAGTTCTG-3′
Wild type	F223Y	5′-CAGAACTCACTCTATGCCACCTACCTCCCCAAGTGGACT-3′ 5′-AGTCCACTTGGGGAGGTAGGTGGCATAGAGTGAGTTCTG-3′
Wild type	L224A	5′-CTCTATGCCACCTTCGCCCCCAAGTGGACTCGC-3′ 5′-GCGAGTCCACTTGGGGGCGAAGGTGGCATAGAG-3′
Wild type	L224I	5′-GAACTCACTCTATGCCACCTTCATCCCCAAGTGGACTCGC-3′ 5′-GCGAGTCCACTTGGGGATGAAGGTGGCATAGAGTGAGTTC-3′
Wild type	P225A	5′-CTCTATGCCACCTTCCTCGCCAAGTGGACTCGCCCCGTG-3′ 5′-CACGGGGCGAGTCCACTTCGCGAGGAAGGTGGCATAGAG-3′
Wild type	K226A	5′-GCCACCTTCCTCCCCGCGTGGACTCGCCCCGTG-3′ 5′-CACGGGGCGAGTCCACGCGGGGAGGAAGGTGGC-3′
Wild type	K226R	5′-TATGCCACCTTCCTCCCCCGGTGGACTCGCCCCGTG-3′ 5′-CACGGGGCGAGTCCACCGGGGGAGGAAGGTGGCATA-3′
Wild type	W227A	5′-GCCACCTTCCTCCCCAAGGCGACTCGCCCCGTGCTG-3′ 5′-CAGCACGGGGCGAGTCGCCTTGGGGAGGAAGGTGGC-3′
Wild type	R229A	5′-ACCTTCCTCCCCAAGTGGACGGCGCCCGTGCTGCCTTTC-3′ 5′-GAAAGGCAGCACGGGCGCCGTCCACTTGGGGAGGAAGGT-3′
Wild type	R229K	5′-ACCTTCCTCCCCAAGTGGACTAAGCCCGTGCTGCCTTTCTGG-3′ 5′-CCAGAAAGGCAGCACGGGCTTAGTCCACTTGGGGAGGAAGGT-3′
Wild type	P230A	5′-CTCCCCAAGTGGACGCGCGCCGTGCTGCCTTTCTGG-3′ 5′-CCAGAAAGGCAGCACGGCGCGCGTCCACTTGGGGAG-3′
Wild type	V231A	5′-CCCAAGTGGACTCGCCCCGCGCTGCCTTTCTGGAAGCGA-3′ 5′-TCGCTTCCAGAAAGGCAGCGCGGGGCGAGTCCACTTGGG-3′
Wild type	V231L	5′-CCCAAGTGGACTCGCCCCTTGCTGCCTTTCTGGAAGCGA-3′ 5′-TCGCTTCCAGAAAGGCAGCAAGGGGCGAGTCCACTTGGG-3′
Wild type	L232A	5′-TGGACTCGCCCCGTGGCGCCTTTCTGGAAGCGATACCTG-3′ 5′-CAGGTATCGCTTCCAGAAAGGCGCCACGGGGCGAGTCCA-3′
Wild type	L232I	5′-GTGGACTCGCCCCGTGATTCCTTTCTGGAAGCGATACCTG-3′ 5′-CAGGTATCGCTTCCAGAAAGGAATCACGGGGCGAGTCCAC-3′
Wild type	P233A	5′-ACTCGCCCCGTGCTGGCTTTCTGGAAGCGATACCTG-3′ 5′-CAGGTATCGCTTCCAGAAAGCCAGCACGGGGCGAGT-3′
Wild type	F234A	5′-CGCCCCGTGCTGCCTGCCTGGAAGCGATACCTGGATGGT-3′ 5′-ACCATCCAGGTATCGCTTCCAGGCAGGCAGCACGGGGCG-3′
Wild type	F234Y	5′-CGCCCCGTGCTGCCTTACTGGAAGCGATACCTGGATGGT-3′ 5′-ACCATCCAGGTATCGCTTCCAGTAAGGCAGCACGGGGCG-3′
Wild type	K236A	5′-GTGCTGCCTTTCTGGGCCCGATACCTGGATGGTTGG-3′ 5′-CCAACCATCCAGGTATCGGGCCCAGAAAGGCAGCAC-3′
Wild type	K236R	5′-CCCGTGCTGCCTTTCTGGCGCCGATACCTGGATGGTTGG-3′ 5′-CCAACCATCCAGGTATCGGCGCCAGAAAGGCAGCACGGG-3′
Wild type	R237A	5′-GTGCTGCCTTTCTGGAAGGCCTACCTGGATGGTTGG-3′ 5′-CCAACCATCCAGGTAGGCCTTCCAGAAAGGCAGCAC-3′
Wild type	R237K	5′-GTGCTGCCTTTCTGGAAGAAGTACTTGGATGGTTGGAATGCC-3′ 5′-GGCATTCCAACCATCCAAGTACTTCTTCCAGAAAGGCAGCAC-3′
F223Y	L219I/F223Y	5′-GGGTTAATGTTCCAGAACTCAATCTATGCCACCTACCTCCCC-3′ 5′-GGGGAGGTAGGTGGCATAGATTGAGTTCTGGAACATTAACCC-3′
L219I/F223Y	L219I/F223Y/F234Y	5′-CGCCCCGTGCTGCCTTACTGGAAGCGATACCTGGATGGT-3′ 5′-ACCATCCAGGTATCGCTTCCAGTAAGGCAGCACGGGGCG-3′
L219I/F223Y/F234Y	L219I/F223Y/F234Y/K236R/R237K	5′-GTGCTGCCTTACTGGCGCAAGTACTTGGATGGTTGGAATGCC-3′ 5′-GGCATTCCAACCATCCAAGTACTTGCGCCAGTAAGGCAGCAC-3′
L219I/F223Y	L219I/F223Y/V231L	5′-CCCAAGTGGACTCGCCCCTTGCTGCCTTTCTGGAAGCGA-3′ 5′-TCGCTTCCAGAAAGGCAGCAAGGGGCGAGTCCACTTGGG-3′
L219I/F223Y/V231L	L219I/F223Y/V231L/F234Y/K236R	5′-CGCCCCTTGCTGCCTTACTGGCGCCGATACCTGGATGGTTGG-3′ 5′-CCAACCATCCAGGTATCGGCGCCAGTAAGGCAGCAAGGGGCG-3′

[a] The mutated nucleotides are underlined.

the enzyme active site (15). Here we describe the effect of mutation of amino acid residues located within the putative F-G loop on subcellular distribution and kinetic parameters for cholesterol 27-hydroxylation of P450 27A1, and we compare mitochondrial P450 27A1 with microsomal P450 7A1.

EXPERIMENTAL PROCEDURES

Site-directed Mutagenesis—This was carried out using an *in vitro* QuikChange™ Site-directed Mutagenesis Kit (Stratagene) according to the instructions. The templates and complementary mutagenic oligonucleotides are shown in Table I. Mutations were confirmed by DNA se-

quencing. The *Kpn*I/*Stu*I fragment of human P450 27A1 containing the mutation was ligated into a *Kpn*I/*Stu*I-digested expression construct containing wild type P450 27A1. For each mutant the region upstream of the *Kpn*I site to beyond the *Stu*I site was sequenced to ensure there were no undesired mutations and to confirm correct ligation.

Subcellular Fractionation of the Mutant P450s in Escherichia coli—E. coli cultures were grown and harvested as described previously (16, 17), and the amount of the functional P450 protein in the *E. coli* cells was assessed by the reduced CO difference spectrum (18). Spheroplasts were prepared by suspending cells in 50% of the original culture volume in 10 mM potassium phosphate buffer (KP_i), pH 7.4, containing 20% glycerol. The cell suspension was incubated with lysozyme (0.5 mg/ml) for 30 min at 4 °C. Spheroplasts were pelleted at 5,000 × *g* for 10 min and then resuspended in 10 mM KP_i, pH 7.4, containing 20% glycerol, 0.5 mM phenylmethylsulfonyl fluoride, 0.5 μg/ml leupeptin, 2 μg/ml aprotinin, and 1 μg/ml pepstatin. After sonication on ice using six 20-s pulses at 1-min intervals, cell debris was removed at 5,000 × *g* (10 min). The supernatant and pellet obtained after subsequent ultracentrifugation at 106,000 × *g* for 60 min were used as cytosolic and membrane fractions, respectively.

Quantification of P450 27A1 Subcellular Distribution—Proteins in subcellular fractions were separated by SDS-PAGE (5 μg of the total protein/lane) and transferred to a nitrocellulose membrane. Western blot analysis was carried out using rabbit antiserum against P450 27A1 and an ECL detection system (Amersham Biosciences) according to the manufacturer's instructions. X-ray films were scanned, and the immunoreactive signal was quantified using NIH Image 1.52 software. Only exposures lying within the film's linear range of sensitivity were used. Statistical analysis was carried out using Microsoft Excel software.

Determination of the Kinetic Parameters for Cholesterol 27-Hydroxylation—Enzymatic activities of wild type and mutated forms of P450 27A1 were determined as described (16, 19) using *E. coli* membrane fractions. The reaction conditions were optimized for the formation of one product only, 27-hydroxycholesterol, linear with time and protein. Reconstituted systems (wild type or mutant) contained varying amounts of P450 (0.01–0.15 μM), 4.0 μM adrenodoxin, 1.0 μM adrenodoxin reductase, cholesterol (2.5–60 μM), [^{3}H]cholesterol (10,500 cpm), 1 mM NADPH and 50 mM KP_i, pH 7.4, in a total volume of 1 ml. The reaction time was 2–4 min. The following modifications, which increased the k_{cat} value 10-fold, were introduced in the enzyme assay; Tween 20 was omitted, and a stock solution of cholesterol (10 mM) was prepared using a 45% aqueous solution of 2-hydroxypropyl-β-cyclodextrin. To determine kinetic parameters for cholesterol 27-hydroxylation, enzymatic activity was measured at a "zero point," when no cold cholesterol was present in the reaction mixture, and the concentration of [^{3}H]cholesterol was very low and equal to 1.9 nM, and in the presence of increasing concentrations of cold cholesterol (2.5–60 μM). The K_m value was calculated from a double-reciprocal plot of a difference between the product formation at a zero point and at a given concentration of cholesterol *versus* concentration of cholesterol. In all studies no more than 15% of radioactive cholesterol was converted at a zero point. To determine the k_{cat} value, we measured the initial velocity of the reaction, v_0, at a zero point when the concentration of the substrate [S] was much lower (less than <1000 times) than the K_m value, using Equation 1,

$$v_o = \frac{\%\ \text{of a product}\cdot[S]}{100\cdot t} \qquad \text{(Eq. 1)}$$

where S is the initial concentration of the substrate, and t is the reaction time. When [S] ≪ K_m (Equation 2),

$$v_o = \left(\frac{k_{cat}}{K_m}\right)\cdot[E]\cdot[S] \qquad \text{(Eq. 2)}$$

where [E] is the concentration of the enzyme (20). The k_{cat} value can thus be determined using Equations 1 and 2 and will be equal to Equation 3,

$$k_{cat} = \frac{\%\ \text{of a product}\cdot K_m}{100\cdot t\cdot[E]} \qquad \text{(Eq. 3)}$$

Substrate and Product Binding Assays—Apparent binding constants (K_d) of P450 27A1 wild type for the substrate, cholesterol, and product, 27-hydroxycholesterol, were determined from the double-reciprocal plot of the ligand-induced spectral change *versus* concentration of free ligand. The latter parameter was calculated using the following equation: $[\text{ligand}_{free}] = [\text{ligand}_{total}] - (\Delta A/\Delta A_{max})[P450]$, where ΔA is a spectral response at a given concentration of the ligand, and ΔA_{max} is the maximal spectral response. The assays were performed using partially purified preparations of P450 27A1 with the specific heme content of 6–8 nmol/mg protein. Titrations with cholesterol (1 μM P450 27A1) and 27-hydroxycholesterol (2 μM P450 27A1) were carried out in 1 ml of 50 mM KP_i, pH 7.2, and 50 mM KP_i, pH 7.2, containing 20% glycerol, respectively. Both ligands were added from a stock solution (1–10 mM) in 45% 2-hydroxypropyl-β-cyclodextrin. After each experiment, P450 content was quantified to confirm that there was no denaturation during titration. Under the experimental conditions used, the apparent K_d of P450 27A1 wild type for the cholesterol was 0.19 μM.

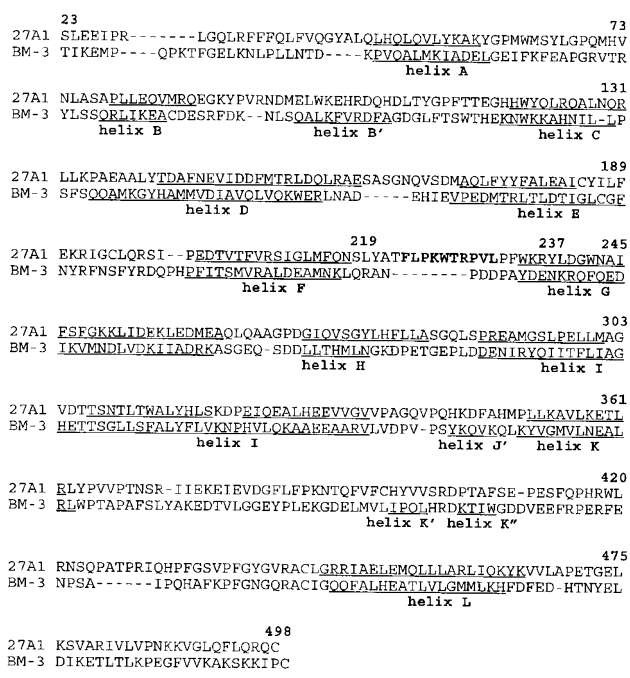

FIG. 1. **Alignment of P450 27A1 with P450 BM-3 (PDB code 1FAG) used for modeling.** *Underlined* regions represent α-helices. Secondary structural elements of P450 27A1 were predicted using the program JPRED, and those of P450 BM-3 were taken from the PDB code 1FAG. The region in *bold* was modeled using constraints extracted from a similar region of PDB code 1QTG (see "Experimental Procedures").

Modeling of P450 27A1—The secondary structure of P450 27A1 was predicted using the JPRED program (jura.ebi.ac.uk:8888/), and modeling templates were identified by searching the protein data base (PDB) with the PsiBLAST (www.ncbi.nlm.nih.gov/BLAST/) and GenTHREADER (bioinf.cs.ucl.ac.uk/psipred/) programs. PsiBLAST indicated that the closest templates in the PDB are P450s BM-3 (PDB code 1FAG), 51 (PDB code 1EA1), and 2C5 (PDB code DT6). The E values were $2e^{-84}$, $6e^{-83}$, and $6e^{-74}$, respectively. GenTHREADER also selected these three targets as HIGH, with a probability of >0.985. For the C-terminal 250 residues, the alignments from GenTHREADER for all three templates agreed well with the secondary structure results from JPRED. However, the alignment in the less conserved N-terminal region was best for P450 BM-3. We thus used the PDB code 1FAG as the template, which is a complex of P450 BM-3 protein with its substrate. The alignment was then hand-corrected in the N terminus of the proteins to improve the concordance with the JPRED secondary structure analysis and the helices in the 1FAG structure. In the final alignment (Fig. 1), 20.41% of the residues were identical between target and template. Distance and angle constraints were extracted with our in-house program EXDIS (21). There were no residues in the template that matched the putative loop area between the F and G helices in P450 27A1. To constrain this region, a BLAST search was done of the PDB using the sequence SLYATFLPKWTRPVL (residues 218–232) from P450 27A1 with the short, exact match option. This indicated a similar loop sequence (Sequence 1) from the structure of the Arc Repressor (PDB code 1QTG) as a suitable template,

```
P450 27A1:  223  FLPKWTRPVL  232
                 FL +W R VL
1QTG:        10  FLNRWPREVL   19
```

SEQUENCE 1

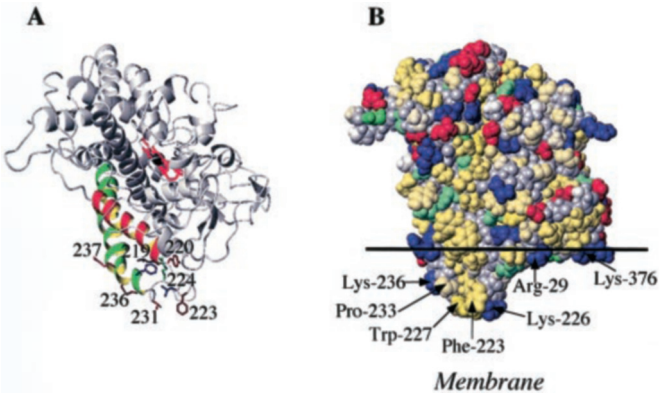

FIG. 2. **Model structure of P450 27A1.** *A*, ribbon diagram showing some of the side chains mutated in this study. The heme group and helix F are in *red*, helix G in *green*, and the residues are *black*, Leu-219; *red*, Tyr-220 and Val-231; *brown*, Phe-223 and Lys-236; *blue*, Leu-224 and Phe-234; *green*, Arg-229; and *pink*, Arg-237. *B*, space-filling Corey-Pauling-Koltien illustration of the model, showing the probable membrane orientation around the (hydrophobic, positively charged) F-G loop. The backbone atoms are *gray*, and the side chains are colored according to the charge (negative, Asp and Glu, *red*; positive, Arg and Lys, *blue*) and hydrophobicity was based on the scale of Fauchere *et al.* (27). Thus, Gly is *white*; Asn, Gln, and His are *light green*; and the other residues are *yellow*, ranging from *dark* (Trp and Phe) to *medium* (Leu, Ile, Val, Met, and Tyr) to *light* (Pro, Thr, and Ala), with Ser *near-white*. The *black line* is drawn to illustrate the hydrophobic surface of the membrane. Images of the model structure were prepared using MolMol (23).

The constraints extracted from this area of the arc repressor (code 1QTG) were then combined with those from P450 BM-3 (code 1FAG). A model was prepared with our (self-correcting distance geometry-based) program DIAMOD (www.scsb.utmb.edu/comp_biol.html/larisa/noah_diamod.html) (22). A Ramachandran plot of the model showed <1% of residues outside the allowed region. To find the approximate position of the heme in the model and to generate constraints for the heme molecule, a structural "best fit" of the model with the template was made with MolMol (www.mol.biol.ethz.ch/wuthrich/software/molmol/) (23). The residues in the model within 8 Å of the heme group of FAG1 in the structural overlay were identified and constraints extracted from the template. These include the covalent bonds between Cys-443 Sγ and Fe^{3+}, as well as longer range constraints to residues Gly-112, Ala-302, Thr-306, Thr-369, Ala-442, Arg-446, and Arg-447. These constraints were combined with the output "corrected" angular and distance constraint list from DIAMOD to generate a model using simulated annealing with the program Sander of the AMBER 6.0 (24) package. AMBER parameters for the heme group were obtained from the Web site pharmacy.man.ac.uk/amber/. The temperature program of the simulated annealing was as follows: steps 0–800, raise target temperature 10 → 200 K; steps 801–1500, raise to 800 K; steps 1501–3500, hold temperature at 800 K; and steps 3501–7000, re-cool to 0 K. The heme molecule in the model generated after this step was not planar. Visual analysis indicated that Tyr-111 was sterically hindering movement of the heme, causing the distortion. Accordingly, in a second simulated annealing step, all constraints for residues 110–112 and those to the heme molecule except the constraint between the heme iron and Cys-443 Sγ were removed from the list. The resulting model showed Tyr-111 at the same position, but the heme group had relaxed to planar geometry.

RESULTS

Modeling and Analysis—Our working model of the P450 27A1 is shown in Fig. 2. Some of the residues studied here, which are probably involved in the F-G loop region, are indicated.

Mutagenesis Strategy—Initially, non-conservative and mainly alanine substitutions were introduced at each position occupied by the hydrophobic, positively charged or proline side chains within the putative F-G loop and the N-terminal part of the G helix in P450 27A1 (residues 219–237, Fig. 1), and the effects on subcellular distribution and kinetic parameters for cholesterol hydroxylation were investigated. Because the observed effects could be the result of conformational changes introduced by non-conservative replacement, additional, conservative substitutions were then generated for each position under the study except for that occupied by the proline residues. Where possible, the conservative mutations reproduced amino acid residues found at the corresponding positions in P450s 27A1 from other species (L219V, V231L, F234Y, and K236R). The K226R substitution reproduces one of the mutations that underlies CTX. Trp-235 and Tyr-238 were studied earlier and the properties of the W235A and Y238A mutants are described elsewhere (15).

Effect of Mutations on Expression Levels in E. coli—As shown in Table II and Fig. 3, conservative and non-conservative substitutions at positions 219, 220, 223, and 236 did not affect the levels of expression of P450 27A1, as assessed by the CO spectra and Western blot analysis. In contrast, both conservative and non-conservative substitutions at positions 224, 226, 229, and 232 reduced by 2–5-fold the amount of the functional P450 form. The decrease in the P450 form of the L224A, L224I, R229K, and L232I mutants correlated with the decrease in the immunoreactive protein on the Western blot, whereas the K226A, K226R, R229A, and L232A mutants showed about 1.5–2.5-fold more immunoreactive protein than the functional P450 form, indicating either reduced stability of the mutant enzyme or a conformational change that affects protein folding and heme binding or both. Conservative substitutions at positions 231, 234, and 237 resulted in the same amounts of functional P450 form as the wild type enzyme, whereas non-conservative alanine mutations decreased the amount of the P450 form to the same extent as the level of the immunoreactive protein. No functional P450 was found in the cells expressing the P225A, W227A, and P233A mutants; however, immunoreactive protein was still detected on a Western blot. In our model structure, both Pro-225 and Pro-233 play important structural roles; Pro-225 is located within one of the turns in the F-G loop, whereas Pro-233 terminates the F-G loop and initiates the helix G. It is likely that the P225A and P233A mutations affected P450 27A1 conformation.

Subcellular Distribution of the Mutant P450s—The wild type P450 27A1 is localized exclusively to the *E. coli* membrane fraction in both low (10 mM KP_i, 20% glycerol) and high (400 mM KP_i, 1 M KCl, 20% glycerol) ionic strength buffers. This P450 is associated with the *E. coli* membrane relatively tightly because only 30–40% of the enzyme can be solubilized from the membrane by using 0.8% sodium cholate. For comparison, ~80% of P450 11A1, another mitochondrial enzyme, can be recovered from the membrane by using 0.5% sodium cholate.

Conservative substitutions of residues that lie on the surface of the P450 27A1 model (Fig. 2), including the L219V, L219I, Y220F, F223Y, L224I, R229K, V231L, F234Y, K236R, and R237K mutations, resulted in appearance from 7.1–21% of P450 27A1 in the cytosol in low ionic strength buffer (Table II and Fig. 3). Supported by the homology model, the subcellular distribution data thus indicate the involvement of Leu-219, Tyr-220, Phe-223, Leu-224, Arg-229, Val-231, Phe-234, Lys-236, and Arg-237 in the interaction with membrane phospholipids. Non-conservative and conservative substitutions of Leu-219 and Tyr-220 provided insight into whether it is the hydrophobicity or the size of the side chain that is important for membrane-protein interactions. In the case of the Leu-219 mutants, the amount of the P450 in the cytosol rose with the increase in size of the replacing amino acid residue (L219N < L219V < L219I). A similar tendency was observed for the Tyr-220 mutants. Replacement of Tyr-220 with Ala or Ser resulted in less cytosolic P450 than mutation to Phe. For Phe-223, substitutions with Ala, Val, and Tyr, which have different

TABLE II
Effect of mutations on expression and subcellular distribution of P450 27A1 in E. coli

P450 27A1	Expression in *E. coli*[a] (nmol/liter)	% in cytosol[b]
Wild type	600–800	0
L219N	Same	7.7 ± 1.4
L219V(as in rabbit P450 27A1)	Same	12.2 ± 0.4
L219I	Same	21.0 ± 1.7
Y220A	Same	7.1 ± 1.2
Y220S	Same	5.9 ± 1.9
Y220F	Same	14.0 ± 0.4
F223A	Same	15.6 ± 3.1
F223L	Same	17.1 ± 1.7
F223Y	Same	12.7 ± 1.3
L224A	↓ ~2-Fold	15.1 ± 1.9
L224I	↓ ~3-Fold	12.0 ± 1.7
P225A	No functional P450	3.6 ± 1.2
K226A	↓ ~3-Fold[c]	15.6 ± 0.8
K226R (underlies CTX)	↓ ~4-Fold[c]	8.6 ± 1.7
W227A	No functional P450	5.6 ± 1.9
R229A	↓ ~10-Fold[c]	2.5 ± 0.5
R229K	↓ ~3-Fold	8.0 ± 1.9
P230A	Same	11.4 ± 3.5
V231A	↓ ~2-Fold	8.6 ± 1.7
V231L (as in pig P450 27A1)	Same	7.1 ± 0.6
L232A	↓ ~3-Fold[c]	11.4 ± 2.0
L232I	↓ ~3-Fold	2.4 ± 0.4
P233A	No functional P450	4.9 ± 1.3
F234A	↓ ~3-Fold	4.6 ± 1.1
F234Y (as in pig P450 27A1)	Same	14.9 ± 1.4
K236A	Same	9.5 ± 2.7
K236R (as in pig P450 27A1)	Same	12.6 ± 1.3
R237A	↓ ~3-Fold	13.5 ± 1.8
R237K	Same	13.9 ± 3.9
L219I/F223Y/F234Y/K236R/R237K	Same	15.6 ± 2.0
L219I/F223Y/V231L/F234Y/K236R	Same	20.6 ± 2.4

[a] Assessed by reduced CO difference spectrum (18).
[b] Assessed by Western blot analysis. Fraction of P450 27A1 in cytosol is expressed as a percentage of the total recovered in the membrane fraction and the cytosol. In all cases, two independent expression experiments were carried out to isolate two sets of membrane fraction and cytosol. SDS-PAGE was then carried out for each set independently, and one or two different gels were run independently for each set following by Western blot analysis. The results represent the average of three to four different Western blot analyses ± S.D.
[c] Spectral analysis showed less functional P450 form than the immunoreactive protein detected by Western blotting.

size and hydrophobicity, led to approximately the same amount of P450 in the cytosol, hereby making interpretation of the results difficult.

Conservative substitution K226R also resulted in a cytosolic P450; however, as discussed earlier, this substitution likely affected either the enzyme stability or conformation. The homology model suggests that the side chain of Lys-226 can form a hydrogen bond with the Phe-223 carbonyl oxygen, and replacement of this side chain may lead to conformational changes in the loop region and consequently weaken the interaction with the membrane. The homology model also provides an explanation of why only small amounts of the L232I mutant were seen in the cytosol. The side chain of Leu-232 is partially buried, and most probably does not contribute significantly to the interaction with membrane phospholipids.

To test whether the F-G loop is the only site of attachment to membrane in P450 27A1, two penta mutants were generated. Multiple mutations resulted in only 15–21% of P450 in the cytosol, amounts comparable with those generated by single substitutions.

Kinetic Parameters for Cholesterol 27-Hydroxylation of the Mutant P450s—As is seen from Table III, conservative and non-conservative substitutions within the F-G loop did not significantly affect the K_m value for cholesterol. The L232A and F234A mutants exhibited the highest, 2.1-fold, increase in K_m. The Y220F and F223L mutants showed the lowest, 2.2-fold, decrease in K_m. However, the k_{cat} values for the mutants varied greatly. On the basis of catalytic properties, the mutants could be arbitrarily placed into two groups. The first group is formed by the L219V, L219I, Y220F, L224A, L224I, R229K, P230A, V231A, V231L, L232I, F234A, F234Y, K236A, K236R, R237A, and R237K mutants. The k_{cat} and catalytic efficiency (k_{cat}/K_m) of these mutants were either unchanged or changed up to 2.9- and 4.6-fold, respectively. The 2.9- and 4.6-fold values were chosen as a cut-off limit for this group of mutants based on the properties of the K226R mutant, a substitution that affects metabolism of cholesterol *in vivo* and results in the disease CTX. Minor effects of both non-conservative and conservative substitutions at positions 224, 231, 234, 236 and 237 (the L224A, L224I, V231A, V231L, F234A, F234Y, K236A, K236R, R237A, and R237K mutants) and non-conservative substitution of Pro-230 to Ala implies that requirements for the size of the side chains at these positions are relaxed for efficient cholesterol hydroxylation.

The second group includes the mutants with significantly (L219N, Y220A, Y220S, F223A, and R229A) and moderately (F223L, F223Y, K226R, and L232A) altered catalytic properties. The L219N, Y220A, and R229A substitutions resulted either in undetectable or very low enzymatic activity, making it difficult to determine the kinetic parameters. The Y220S and F223A replacements decreased the catalytic efficiency more than 50-fold, and the K226R substitution led to a 4.6-fold decrease in catalytic efficiency. The k_{cat} of the F223L, F223Y, and L232A was changed 3.1–3.8-fold. However, the catalytic efficiency was changed only up to 1.8-fold because of the simultaneous change of the K_m. In contrast to the R229A, K226R, and L232A mutants, undetectable or extremely low enzymatic activity of the L219N, Y220A, Y220S, and F223A mutants and the decreased k_{cat} of the F223L and F223Y mutants are not the result of structural perturbations around the heme, because the membrane fractions of these mutants showed a large peak at 450 nm and a small peak at 420 nm in the reduced CO difference spectrum (Fig. 4), indicating retention of the integrity of the P450 heme environment. The data therefore indicate that size and polarity of the side chains at positions 219, 220, and 223 are crucial for the efficient catalysis of cholesterol.

DISCUSSION

The results obtained in this study indicate that the putative F-G loop and the N-terminal part of the putative helix G (residues 219–237) are involved in the association with membrane in P450 27A1. Analysis of the effects of amino acid substitutions on expression and subcellular distribution of mutant enzymes and examination of the homology model allowed identification of residues that are likely to participate in the interaction with membrane phospholipids (Leu-219, Tyr-220, Phe-223, Leu-224, Arg-229, Val-231, Phe-234, Lys-236, and Lys-237) and residues whose mutations might cause structural

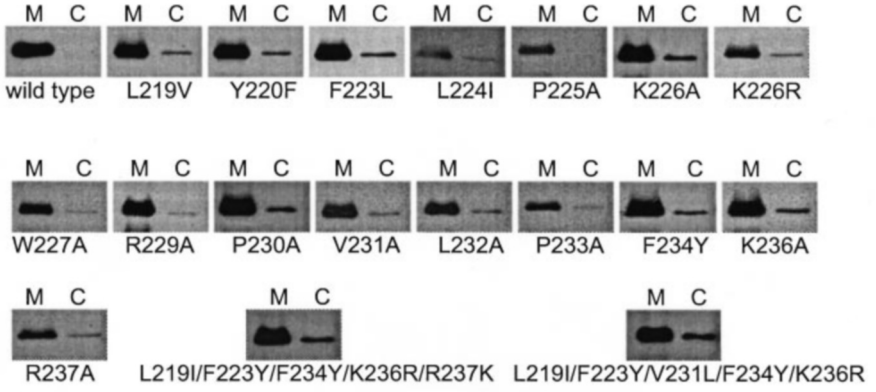

FIG. 3. **Representative Western blots showing subcellular distribution of P450 27A1 wild type and some of the mutants in *E. coli*.** *M* and *C* indicate the membrane fraction and cytosol, respectively.

rearrangements, resulting in a change of the shape of the putative F-G loop and membrane binding properties (Pro-225, Lys-226, Trp-227, and Pro-233). The putative F-G loop is predicted to contribute to membrane association in microsomal P450s (10, 11) and shown to contain residues involved in the interaction with the lipid bilayer in microsomal P450s 2B1, 2C5, and 7A1 (12–14). The present work is the first study showing that the putative F-G loop and the N-terminal part of the putative G helix are also the sites of membrane attachment in mitochondrial P450 27A1. As this region is amphipathic and about the same size in different mitochondrial P450s (15), it is very likely that the putative F-G loop and a part of the helix G are also involved in membrane binding in other mitochondrial P450s. Thus, microsomal and mitochondrial P450s appear to have an overlapping membrane-binding site. This finding supports the notion that mitochondrial P450s most probably arose from mistargeting of microsomal enzymes during evolution (26). Introducing five different mutations simultaneously in the loop had no more effect on membrane attachment than a single mutation suggesting that there are additional site(s) of association with the membrane in P450 27A1. Weakening of the membrane-protein interactions in the putative F-G loop may lead to a tighter binding to the membrane at the other site(s).

Previously, we have shown that conservative and nonconservative substitutions of the three residues within the putative F-G loop, which forms a part of the enzyme-membrane interface in microsomal cholesterol hydroxylating P450 7A1, decreased significantly the K_m value for cholesterol but did not alter the apparent K_d value (14). We proposed that these residues are adjacent to the entry of the substrate access channel and that they participate in substrate recognition, which involves initial docking of cholesterol and determines orientation of the substrate as it enters the substrate access channel and then the enzyme active site (14). In mitochondrial cholesterol hydroxylating P450 27A1, mutations within the putative F-G loop did not significantly affect the K_m, indicating that either cholesterol is not recognized by the surface residues in P450 27A1 or the putative F-G loop is not the site where cholesterol recognition occurs. The K_m value for cholesterol of P450 27A1 (7.0 μM) is more than 30-fold higher than the K_d value (0.19 μM), indicating that binding and release of the substrate is slower than product formation and release (k_{cat}) and are thus the rate-limiting steps in the 27-hydroxylation of cholesterol (Table IV). This is in contrast to P450 7A1, the K_m and K_d values of which are similar (6.9 μM and 9.5 μM, respectively). Possibly, these two P450s have different mechanisms for substrate recruitment and retaining in the active site.

P450s 7A and 27A1 are also different in terms of their catalytic efficiencies because the k_{cat} value of P450 7A1 is more

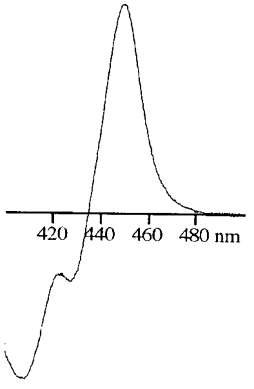

FIG. 4. **A typical CO-reduced difference spectrum exhibited by the membrane fractions of the L219N, Y220A,Y220S, F223A, F223L, and F223Y mutants.**

than 20-fold higher than that of P450 27A1 (349 *versus* 15.6 min^{-1}), whereas the K_m values are approximately the same (Table IV). Non-conservative substitutions of Leu-219, Tyr-220, and Phe-223, the side chains which are likely involved in the interaction with membrane phospholipids, significantly impaired catalytic activity of mutant P450s. This finding raises a question as to how the mutations of the surface residues located outside the enzyme active site influence the catalysis inside the buried active site. There are two possible explanations in our opinion. The first is that weakening of the membrane-protein interactions increases water access to the substrate access channel and enzyme active site. Water molecules can serve as the proton donor for catalysis, and changes in the active site solvation may affect the proton-transfer pathway to bound oxygen and consequently catalysis. The second explanation is that alteration of the membrane-protein interactions slows down exit of product, thus decreasing the k_{cat}. To test whether the mutations affected product binding, we tried to determine the apparent K_d value for 27-hydroxycholesterol by using a spectral binding assay. Unfortunately, the spectral shift of the wild type P450 27A1 induced by 27-hydroxycholesterol was very low, thereby precluding a reliable determination of the constant.

Kinetic differences between P450s 27A1 and 7A1 are likely to reflect different physiological requirements for the two enzymes. Up to 400 mg of cholesterol is degraded daily to bile acids through the classical bile acid biosynthetic pathway in which P450 7A1 catalyzes the first and rate-limiting step (3), and only about 4% of cholesterol (16 mg) is converted to bile acids through the alternative (extrahepatic) bile acid pathway initiated by the P450 27A1 (26). Because of the high quantities of cholesterol that must be metabolized, P450 7A1 should be a

TABLE III
Effect of mutations on kinetic properties of P450 27A1

Kinetic parameters for 27-hydroxylation of cholesterol were determined as described under "Experimental Procedures." The results are the mean ± S.D. of three to four experiments.

P450 27A1	K_m μM	k_{cat} min^{-1}	$k_{cat}/K_m/min^{-1} \cdot \mu M^{-1}$
Wild type	7.0 ± 1.0	15.8 ± 2.6	2.2 ± 0.3
L219N		Undetectable activity	
L219V (as in rabbit P450 27A1)	12.1 ± 0.3	28.3 ± 2.5	2.3 ± 0.3
L219I	7.2 ± 0.8	24.7 ± 4.5	3.4 ± 0.3
Y220A		Undetectable activity	
Y220S	6.9 ± 1.6	0.3 ± 0.1	0.04 ± 0.01
Y220F	3.2 ± 0.7	8.7 ± 1.9	2.7 ± 0.1
F223A	19.8 ± 6.0	0.9 ± 0.3	0.04 ± 0.003
F223L	3.2 ± 0.5	4.2 ± 0.4	1.3 ± 0.1
F223Y	4.0 ± 0.5	4.9 ± 0.9	1.2 ± 0.1
L224A	5.2 ± 0.4	9.4 ± 0.2	1.8 ± 0.1
L224I	12.0 ± 0.1	13.8 ± 2.2	1.1 ± 0.2
P225A		No functional P450	
K226A	13.4 ± 1.1	38.3 ± 4.2	2.9 ± 0.1
K226R (underlies CTX)	11.3 ± 0.5	5.4 ± 0.1	0.48 ± 0.01
W227A		No functional P450	
R229A		Very low activity	
R229K	13.6 ± 2.1	29.9 ± 1.2	2.2 ± 0.2
P230A	11.1 ± 0.9	25.7 ± 1.9	2.3 ± 0.01
V231A	8.6 ± 1.4	22.0 ± 2.3	2.6 ± 0.2
V231L (as in pig P450 27A1)	6.6 ± 0.6	21.0 ± 0.9	3.2 ± 0.2
L232A	14.6 ± 1.2	49.7 ± 5.8	3.4 ± 0.4
L232I	13.8 ± 3.7	31.6 ± 6.0	2.4 ± 0.6
P233A		No functional P450	
F234A	14.5 ± 0.9	22.1 ± 3.0	1.53 ± 0.1
F234Y (as in pig P450 27A1)	9.9 ± 1.4	27.8 ± 1.6	2.9 ± 0.5
K236A	6.6 ± 0.6	13.7 ± 1.2	2.1 ± 0.3
K236R (as in pig P450 27A1)	12.6 ± 1.2	32.0 ± 6.1	2.5 ± 0.3
R237A	7.9 ± 1.2	34.8 ± 7.1	4.4 ± 0.2
R237K	11.3 ± 1.1	27.2 ± 3.1	2.5 ± 0.5
L219I/F223Y/F234Y/K236R/R237K		Not determined	
L219I/F223Y/V231L/F234Y/K236R		Not determined	

TABLE IV
Comparison of kinetic and cholesterol binding properties of P450s 7A1 and 27A1

P450	K_d^s	K_m	k_{cat}	k_{cat}/K_m	Source
	μM		min^{-1}	min^{-1} μM^{-1}	
7A1 (M[a])	ND[b]	14.0	349	24.9	14
7A1 (P.P.[a])	9.5	6.9	111	16.1	14
27A1 (M)	ND	7.0	15.8	2.3	Present work
27A1 (P.P.)	0.19	ND	ND	ND	Present work

[a] M, membrane fraction; P.P., partially purified enzyme.
[b] ND, not determined.

more efficient enzyme than P450 27A1.

To summarize, the novelty of the present work is that it provides insight into membrane topology of mitochondrial P450s by mapping for the first time the secondary structural elements involved in binding to the membrane, presents the first experimental verification of the concept that microsomal and mitochondrial P450s have a similar mode of association with the membrane (8, 9), establishes that intact membrane-protein interactions are important for efficient catalysis in P450s, and ascertains kinetic differences between P450s 7A1 and 27A1, two major enzymes in degradation of cholesterol.

Acknowledgments—Oligonucleotide synthesis and DNA sequencing were carried out by the Recombinant DNA Laboratory of the National Institute of Environmental Health Sciences Center and the Protein Chemistry Laboratory, respectively, at the University of Texas Medical Branch.

REFERENCES

1. Schwarz, M., Lund, E. G., and Russell, D. W. (1998) *Curr. Opin. Lipidol.* **9,** 1–6
2. Myant, N. B., and Mitropolus, K. A. (1997) *J. Lipid Res.* **18,** 135–153
3. Russell, D. W., and Setchell, K. D. R. (1992) *Biochemistry* **31,** 4737–4749
4. Anderson, K. E., Kok, E., and Javitt, N. B. (1972) *J. Clin. Invest.* **51,** 112–117
5. Björkhem, I. (1992) *J. Lipid Res.* **33,** 455–471
6. Cali, J. J., Hsieh, C.-L., Francke, U., and Russell, D. W. (1991) *J. Biol. Chem.* **266,** 7779–7783
7. Verrips, A., Hoefsloot, L. H., Steenbergen, G. C. H., Theelen, J. P., Wevers, R. A., Gabreels, F. J. M., Englen, B. G. M., and Heuvel, L. P. W. J. (2000) *Brain* **123,** 908–919
8. Wachenfeldt, C., and Johnson, E. F. (1995) in *Cytochrome P450: Structure, Mechanism, and Biochemistry* (Ortiz de Montellano, P. R., ed) 2nd Ed., pp. 183–244, Plenum Publishing Corp., New York
9. Williams, P. A., Cosme, J., Sridhar, V., Johnson, E. F., and McRee, D. E. (2000) *Mol. Cell* **5,** 121–131
10. Graham-Lorence, S., Amarneh, B., White, R. E., Peterson, J. A., and Simpson, E. R. (1995) *Protein Sci.* **4,** 1065–1080

11. Peterson, J. A., and Graham, S. E. (1998) *Structure* **6,** 1079–1085
12. De Lemos-Chiarandini, C., Frey, A. B., Sabatini, D. D., and Kreibich, G. (1987) J. *Cell Biol.* **104,** 209–219
13. Cosme, J., and Johnson, E. F. (2000) *J. Biol. Chem.* **275,** 2545–2553
14. Nakayama, K., Puchkaev, A., and Pikuleva, I. (2001) *J. Biol. Chem.* **276,** 31459–31465
15. Pikuleva, I. A., Puchkaev, A., and Bjorkhem, I. (2001) *Biochemistry* **40,** 7621–7629
16. Pikuleva, I. A., Björkhem, I., and Waterman, M. R. (1997) *Arch. Biochem. Biophys.* **343,** 123–130
17. Pikuleva, I. A., Cao, C., and Waterman, M. (1999) *J. Biol. Chem.* **274,** 2045–2052
18. Omura, T., and Sato, R. (1964) *J. Biol. Chem.* **239,** 2370–2378
19. Pikuleva, I. A., Babiker, A., Waterman, M. R., and Björkhem, I. (1998) *J. Biol. Chem.* **273,** 18153–18160
20. Voet, D., and Voet, J. G. (1990) *Biochemistry*, p. 338, John Wiley & Sons, Inc., New York
21. Soman, K. V., Schein, C. H., Zhu, H, and Braun, W. (2001) in *Nuclease Methods and Protocols* (Schein, C. H., ed) Vol. 160, pp. 263–286, Humana Press Inc., Totowa, NJ
22. Mumenthaler, C., and Braun, W. (1995) *Protein Sci.* **4,** 863–871
23. Koradi, R., Billeter, M., and Wüthrich, K. (1996) *J. Mol. Graphics* **14,** 51–55
24. Pearlman, D. A., Case, D. A., Caldwell, J. W., Ross, W. R., Cheatham, T. E., III, DeBolt, S., Ferguson, D., Seibel, G., and Kollman, P. (1995) *Comp. Phys. Commun.* **91,** 1–41
25. Nelson, D. R. (1998) *Comp. Biochem. Physiol.* **121,** 15–22
26. Lund, E., Andersson, O., Zhang, J., Babiker, A., Ahlborg, G., Diczfalusy, U., Einarsson, K., Sjovall, J., and Bjorkhem, I. (1996) *Arterioscler. Thromb. Vasc. Biol.* **16,** 208–212
27. Fauchere, J., Charton, M., Kier, L. B., Verloop, A., and Pliska, V. (1988) *Int. J. Pept. Protein Res.* **32,** 269–278